Technical Report No. TRL-102

BIAS CORRECTIONS IN TURBULENCE MEASUREMENTS BY THE LASER DOPPLER ANEMOMETER*

by

P. Buchhave** and W. K. George, Jr.

Turbulence Research Laboratory
Faculty of Engineering and Applied Sciences
State University of New York at Buffalo
Buffalo, New York 14214

July 1978

* To be published in: Proceedings of the Third Workshop on Laser Doppler Anemometry, July 11-13, 1978, Purdue University, W. Lafayette, Indiana

** On leave from DISA Elektronik, Copenhagen, Denmark

Acknowledgements

Preben Buchhave acknowledges the support of the Danish Natural Science Research Council and the Danish Council for Scientific and Industrial Research.

William K. George and Preben Buchhave acknowledge the support of the U.S. National Science Foundation, Meteorology Program under Grant Number ATM-76-02157 and the Fluid Mechanics Program under Grant ENG-76-17466.

The authors also acknowledge the support of DISA Electronics Inc. for providing part of the equipment on load and for help with installation and operation of the equipment.

BIAS CORRECTIONS IN TURBULENCE MEASUREMENTS BY THE LASER DOPPLER ANEMOMETER

PREBEN BUCHHAVE*and WILLIAM K. GEORGE, JR.
Turbulence Research Laboratory
Faculty of Engineering and Applied Science

State University of New York at Buffalo
Buffalo, New York 14214

*On leave from DISA Elektronik

1. Introduction

This paper describes work presently underway at the Turbulence Research Laboratory, Faculty of Engineering and Applied Sciences, State University of New York at Buffalo. The object of this program is partly to develop correct data analysis algorithms and software for bias-free estimation of statistical flow quantities based on randomly arriving LDA-counter data, partly to serve as a pilot program for the design of a larger experimental facility for jet noise studies, now in its initial phase.

This paper is only to be considered a "work in progress" report since measurements and software development on this particular project are still in their initial phase

The basic philosophy behind the development of data analysis programs is that the so-called individual realization LDA bias or statistical bias is not a mysterious and elusive property of some types of flow, but that the effect is always present in individual realization anemometry, and that the "bias" is only a result of incorrect data processing. Also, that the underlying sampling mechanism causing the bias (when data are treated incorrectly) is not something to try to avoid, but rather the "natural" way in which individual realization anemometers work, and that indeed the individual realization or single burst data collection is in many cases a desirable feature of such instruments, which may lead to new insight or alternative methods of measuring dynamic flow quantities.

To illustrate this we mention just a few of these possibilities: Seeding only one of the constituents in a turbulent mixing process, e.g. a jet issuing into an unseeded environment or vice-versa, presents a way of conditionally sampling fluid elements originally present in only one of the media. Also, the randomly sampled data provided by the individual realization anemometer allows alias-free spectral estimation and a time resolution beyond the usual Nyquist criterion.

The algorithms required for correct data processing of individual realization data are not more complicated than those used in normal arithmetic averaging and, apart from the requirement of being able to transfer more bits of information per measured data point, the hardware needed for bias-free data collection is not much more complicated than previously used LDA-counter circuitry.

The theoretical background for the individual realization data processing

biased and unbiased LDA-data processing can be found in Reference 2.

2. Experimental Setup and Data Collection Equipment

The experimental set-up is shown in Figure 1. The flow is a 3" diameter free jet in air. The air flow passes through a 12" diameter plenum chamber containing honey-comb and a number of screens. The flow is accelerated through a 16:1 contraction having a profile of matched cubics. The Laser anemometer is a DISA X-type optical system operating in forward scatter mode. The Laser is a Spectra-Physics 15 mW He-Ne laser Model 125. The optics defines a measuring volume approximately 0.1 mm in diameter and approximately 0.2 mm in length, located approximately 300 mm from the optical components. The whole optical system can be traversed in two directions in the horizontal plane. The whole environment around the jet and the optical system can be sealed off allowing uniform seeding of the whole flow field. Droplets (1-3μm dia.) of a 50:50 pct mixture of glycerin and water were used as seeding. The optical system includes a Bragg cell frequency shift module operating at a constant frequency of 40 MHz. Electronic mixing with a local oscillator in the signal processing equipment (DISA 55N10 Dual-channel Frequency Shifter)phase-locked to the Bragg cell driver allows convenient selection of the effective frequency shift from 10 KHz to 10 MHz.

The signal processing equipment is composed of standard DISA LDA components and is shown in Figure 2. The rack contains from the top two 55L90a counters, a 55N10 Frequency Shifter, a 56G20 Interface and Buffer, a DEC LSI-11 mini-computer and a DEC DX-11 Dual Floppy Disk System. A block diagram is shown in Figure 3. The digital output from the counter is transferred to the Interface and Buffer, which handles up to eight parallel 16-bit input words and eight parallel, 16-bit output words. Two of the interface output lines are used to communicate with the LSI-11 minicomputer. The computer is controlled through a Beehive B-100 terminal and storage is provided by the DEC DX-11 Dual Floppy Disk System.

The Interface and Buffer contain a backplane with a number of print sockets and can be built up to the required complexity by inserting optional prints. The main ingredient is an input logic and buffer card, which handles incoming data, marks the data words so the source can later be identified, and stores the data in the 500 word SILO-type memory. The buffer can accept asynchroneous data with a time spacing of only 1μs (or by replacement of memory elements with somewhat more expensive, but pin-for-pin compatible chips, a spacing of only 70 ns). A high data reception rate is required by the interface to take advantage of the short time lags inherent in the random sampling of the LDA, especially if more channels are used. The function of the buffer is primarily to allow reception of asynchroneous data and subsequent transmission to the computer. The buffer can be expanded if needed to 2000 words by insertion of additional memory cards with no change in logic circuitry. The function of the interface is controlled by the control logic card, and an output demultiplexer card allows communication through the remaining six 16-bit channels (in addition to the two occupied by the computer) for controlling external devices (flow parameters, traversing mechanisms, or other).

The LDA-counter mode of operation is an important factor in the data processing and is explained with reference to table 1. The DISA 55L90a counter may operate in four modes of which one (the fourth) is primarily of interest in time-of-flight measurements.

Mode-1 is the most common mode of operation of conventional LDA-counters. A measurement is initiated when the signal exceeds the fringe counter Schmidt trigger level. The first zero-crossing enables the counter and counting of clock oscillator pulses continues through the following eight zero-crossings if the counter is not reset by a detected error condition by the validation circuits (in which case the counter is immediately reset). The immediate reset allows

the highest possible data rate and ensures that a burst is measured even if a fault should occur in the initial phase of the burst. In mode-1 new measurements continue based on eight zero-crossings throughout the burst as long as Doppler periods exceeding the Schmidt trigger level are available. The measurement is checked by a 5:8 comparator circuit and three other validation schemes (burst amplitude exceeding preset level, measured velocity below preset range minimum and burst envelope dip detected by two-level sequency detector).

Mode-3 bases the measurement on the total number of periods in the burst (from 2 to 256), only one measurement is output per burst, and in addition to the velocity output the number of zero-crossings measured per burst, N_z, is also available in binary form at the output. However, in this mode the 5:8 comparison is not active and the counter is thus somewhat more sensitive to noise in this mode. The "velocity" output is based on a variable number of zero crossings and must therefore be "normalized" relative to N_z.

Mode-2 combines the positive features of mode-1 and mode-3. The measurement is still based on eight zero crossings, the 5:8 comparison is active, but only one measurement is made per burst and the total number of zero crossings is available at the output. Unless the S/N is high mode-2 works better than mode-3, which can give many data points based on only 2,3 or a low number of zero-crossings. Mode-3 may be somewhat less sensitive to the finite fringe number angular effect described later if frequency shift is not used.

In the measurements described here only mode-2 was employed and variable frequency shift was always available.

3. Data Processing

In Reference 1 and 2 it is shown that the digital samples measured in individual realization anemometers can be used to form the correct time-averaged statistical quantities of the flow provided each realization enters the time integral only during the time the particle is present in the measuring volume. This forms the basis for the so-called residence-time weighted averaging in which the measured residence time of each sample enters the formulas as a weighting factor to be applied to each individual data point. The resulting formulas for the time-averaged mean and mean-square velocity are given by:

Residence-time weighting

$$U = \frac{\sum_i u_i \Delta t_i}{\sum_i \Delta t_i}$$

$$\overline{u'^2} = \frac{\sum_i (u_i - U)^2 \Delta t_i}{\sum_i \Delta t_i}$$

where Δt_i is the measured residence time of the i^{th} realization. Throughout the paper the velocity vector is denoted by $\underline{u} = (u,v,w)$ and $\underline{U} = (U,V,W)$ and $\underline{u}' = (u',v',w')$ denote mean and fluctuating components respectively.

The corresponding formulas for the straight arithmetic averaging, which are only correct for equidistantly sampled data, but which give bias-errors when applied to individual realization anemometers, are:

Arithmetic averaging:

$$U_{AR} = \frac{\sum_i u_i}{N}$$

$$\overline{u'^2_{AR}} = \frac{\sum_i (u_i - U_{AR})^2}{N}$$

and the algorithms using the one-dimensional correction proposed originally by McLaughlin and Tiederman (Reference 3), which provide an approximate bias-correction at low turbulence intensities, are:

One-dimensional correction:

$$U_{1D} = \frac{\sum_i u_i |u_i|^{-1}}{\sum_i |u_i|^{-1}}$$

$$\overline{u'^2_{ID}} = \frac{\sum_i (u_i - U_{1D})^2 |u_i|^{-1}}{\sum_i |u_i|^{-1}}$$

In Reference 1 and 2 it is shown that the residence-time weighted data provides the correct answer assuming statistically uniform spatial particle distribution throughout the flow, and provided the measuring volume has the same effective size independent of flow direction. In other words, the finite fringe number effect due to the fact that the LDA-signal processor requires a minimum number of fringes for processing must be eliminated by the use of frequency shift or by other methods. Note that when the finite fringe number effect is negligible the measuring volume may have any shape (ellipsoidal or other) without causing any bias-effects.

A convenient, frequency independent method of measuring the residence time is provided by the binary output of the total number of zero-crossings N_z in a burst in conjunction with the measured frequency, f_m. The residence time is simply given by:

$$\Delta t_i = \frac{N_{z,i}}{f_{m,i}}$$

where $f_m = f_o + f_s$ is the sum of the Doppler frequency and the applied frequency shift. This formula is valid with or without frequency shift.

The angular effects due to the requirement of a finite number of zero-crossings was first studied in Reference 4 for arithmetic averaging (non-corrected data) and 1-D weighted data. These effects are briefly described with reference to Figure 4 and 5. Figure 4 shows the effective cross-sectional area of the measuring volume within which particle trajectories of direction $\underline{u}/|\underline{u}|$ will result in an output from the signal processor. This cross-sectional area is a function of the direction and of the ratio Q of the maximum number of fringes in the measuring volume N_f (particle trajectory along the x-axis) to the minimum number N_e required by the processor: $Q = N_e/N_f$, as shown in the figure. The limit $Q \to 0$, which corresponds to the case considered by McLaughlin and

Tiederman, may be approached by requiring only a small N_e (such as two in mode-3) or by adding enough frequency shift so that a particle always produces more than N_e zero-crossings independent of velocity magnitude and direction.

The biasing effects resulting from arithmetic and 1-D weighted averaging were also considered in Reference 4 for various flow situations. Figure 5 shows the computed error in mean and mean-square velocity assuming a three-dimensional isotropic, Gaussian turbulence as a function of the turbulence intensity. Correctly averaged data would of course result in points on the x-axis. It should be noted that the finite fringe number effect and the over-compensation introduced by the 1-D correction act in opposite directions and for a certain value of Q (Q≈0.2 for the particular flow considered in this example, corresponding to e.g. 8 fringes required of a maximum of 40) nearly cancel even for large turbulence intensity. This may explain why some authors have got surprisingly good results with the approximative 1-D correction.

4. Measurements

Mean and mean-square velocities have been measured along the axis and across the jet at various locations. The data have been computed using the three sets of algorithms shown in the previous section for various amounts of frequency shift. Some of the data are presented in the following figures.

The measurements have been carried out all the way through the jet to regions at the edge of the jet, where the turbulence intensity is very high. The data were extremely stable as long as sufficiently long averaging time was used in order to form averages over many integral time scales of the flow. Ensembles of 2000 or more data points were used, and the variance of the measured data points was only a few percent.

Figure 6 shows the measured mean values using the three different averaging techniques in a scan along the axis of the jet, and the percentage difference between the arithmetic and 1-D corrected data relative to the residence time weighted results. Figure 7 shows similar results for a transverse scan at X/D = 5.3. The difference in the two figures shows the influence of frequency shift. The frequency shift used obtaining the data shown in Figure 7 was sufficient to eliminate angular dependence due to the finite fringe number effect.

Unfortunately it has not yet been possible to provide an absolute reference by which to firmly establish the validity of the residence-time weighted results in a three-dimensional, highly turbulent flow. Presently it is only possible to establish the fact that large differences occur in using the three mentioned averaging methods, and that the measured differences conform to the trend suggested by previous analysis. The influence of frequency shift also confirms the trend expected from that analysis. From Figure 7C it is evident that the opposite trends of the angular dependence and the 1-D compensation help reduce the difference between the residence-time weighted data and the 1-D corrected data whereas a larger difference exists in the case shown in Figure 7B where the angular dependence has been minimized by frequency shift.

More detailed measurements will be published in Reference 2 and it will also be attempted to establish a reference to an unbiased measurement of sufficient accuracy to allow comparison with the residence-time weighted data.

5. Autocorrelation Function

The theory of residence-time weighting of statistical quantities involving more than one realization is also developed in Reference 1 and 2. There it is shown that the time-averaged autocorrelation function from individual realization anemometers can be computed by only integrating the realizations while both are "on" at the same time. The resulting expression for the time-averaged correlation function from individual realizations becomes:

$$\sum_{i<j} \Delta t_{ij}$$

where $t_j - t_i$ are the actually occurring lags between pairs of realizations and $\Delta\tau$ is the slot-width for the slotted time-average autocorrelation estimator (see Reference 5 and 6). Δt_{ij} is the "overlap-time", i.e. the time in which both the realization u_j and t_{ij} and the delayed realization u_i and $t_i+\tau$ are present simultaneously.

It can further be shown that the estimator Equation (5.1) is equivalent to the following expression based directly on the measured residence times:

$$R(n\Delta\tau) = \frac{\sum_{i<j} u_i u_j \Delta t_i \Delta t_j}{\sum_{i<j} \Delta t_i \Delta t_j} \qquad (n-1/2)\ \Delta\tau \leq t_j - t_i < (n+1/2)\Delta\tau \qquad (5.2)$$

This expression provides an autocorrelation estimator based on the measured values of velocity and residence time, which is equivalent to the time-averaged autocorrelation function (i.e. bias-free) provided, as before, the particle distribution is statistically uniform throughout space and the finite fringe number effect has been eliminated. Note, that this estimator does not contain self-products and thus is in accordance with the estimators developed by Mayo (Ref. 5) and Gaster and Roberts (Ref. 6).

The estimator Equation (5.2) and similar estimators based on arithmetic averaging and 1-D weighted data have been implemented on the data processing equipment described here, and some measurements have been made both in the centerline of the jet and in the highly turbulent region off-axis. Preliminary results indicate an appreciable difference in results obtained using the three different methods, even at the jet centerline. Figure 8 shows typical results obtained at the jet centerline at X/D=5.3. The two curves show the result of arithmetic averaging compared to residence-time weighted data. Evidently the influence of the bias-errors is most marked for large time lags.

Further work on the influence of individual realization bias on autocorrelations and spectra is in progress and will be presented in Reference 2.

References

1. P. Buchhave, W.K. George, Jr. and J.L. Lumley, "The Measurement of Turbulence with the Laser Doppler Anemometer", Prepared for publication in Annual Review of Fluid Mechanics, Annual Reviews, Inc., Palo Alto, California, 94306 (Van Dyke and Wehausen, Co-editors). Also issued as TRL-101 by Turbulence Research Laboratory, State University of New York at Buffalo.
2. P. Buchhave (1978) "Errors and Correction Methods in Turbulence Measurements with the LDA", Ph.D. Thesis, Department of Mechanical Engineering, State University of New York at Buffalo, Buffalo, New York.
3. D.K. McLaughlin and W.K. Tiederman (1973), "Biasing Correction for Individual Realization of Laser Anemometer Measurements in Turbulent Flows", Phys. of Fluids, 16, pp. 2082-2088.
4. P. Buchhave (1976), "Biasing Errors in Individual Particle Measurements with the LDA-Counter Signal Processor". In proceedings of the LDA-Symposium Copenhagen, 1975: pp. 258-278. Copenhagen: PO Box 70, 1740 Skovlunde, Denmark. 736 pp.
5. W.T. Mayo, M.T. Shay and S. Riter (1924) "The Development of New Digital Data Processing Techniques for Turbulence Measurements with a Laser Velocimeter". Final Report (AEDC-TR-74-53), USAF Contract Co. F40600-73-C-003, August 1974.
6. M. Gaster and T.B. Roberts (1975) "Spectral Analysis of Randomly Sampled Signals". J. Inst. Maths. Applic., 15, 195-216.

TABLE 1. DISA 55L95 COUNTER MODES

MODE	N_z	VALIDATION	OPERATION	OUTPUT
1 CONTINUOUS	8	5:8 + 3	CONTINUOUS	V, T
2 COMBINED	8	5:8 + 3	ONE PER BURST	V, T, N_b
3 TOTAL BURST	N_b	- + 3	ONE PER BURST	"V", T, N_b
4 "STOP WATCH"	2	- + 3	CONTINUOUS	1/ T, T

N_z = NUMBER OF ZERO-CROSSINGS TIMED

N_f = NUMBER OF FRINGES IN MEASURING VOLUME

N_S = NUMBER OF PERIODS ADDED BY FREQUENCY SHIFT

N_b = NUMBER OF PERIODS IN MEASURED BURST = $N_f + N_s$

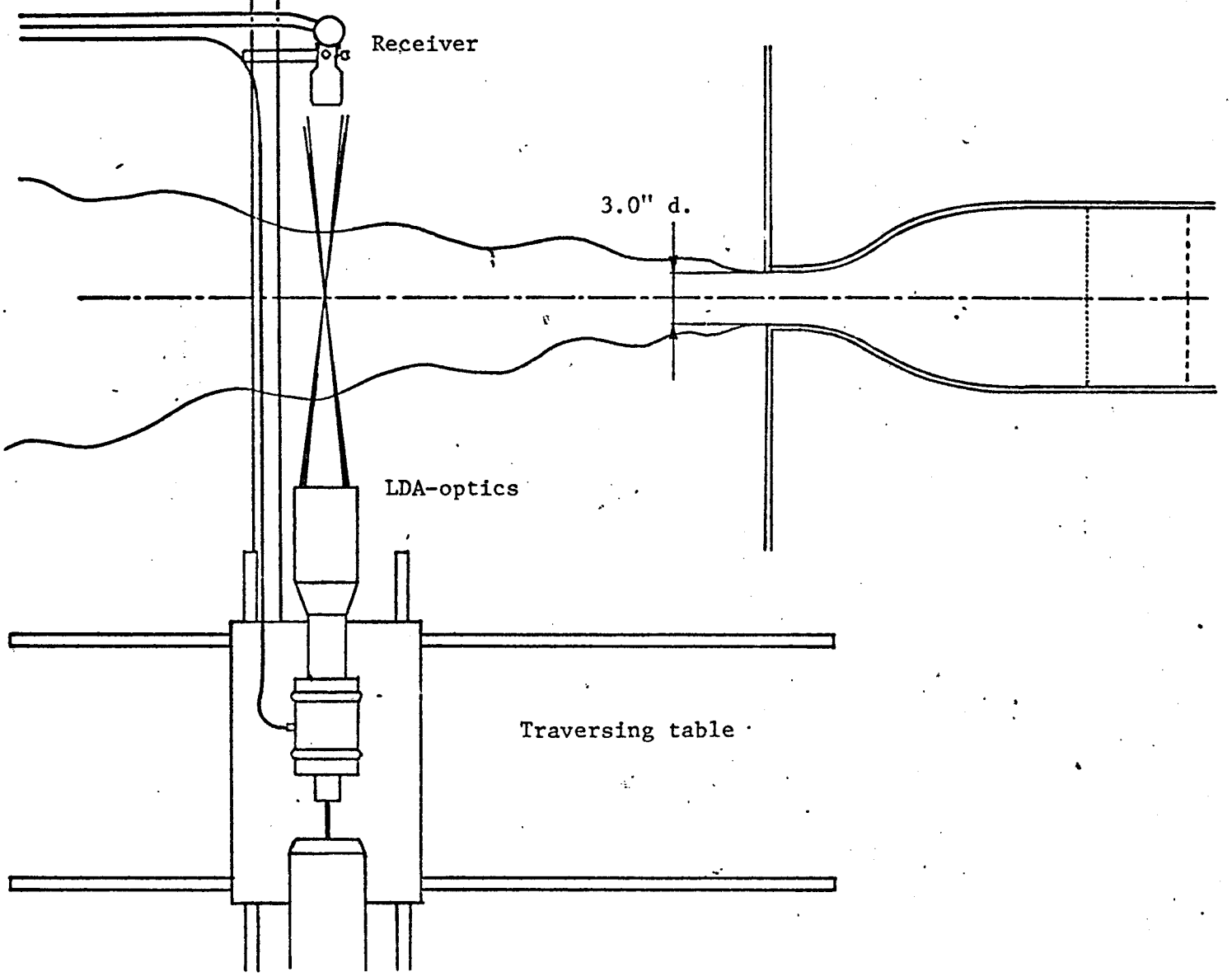

Figure 1. Experimental setup.

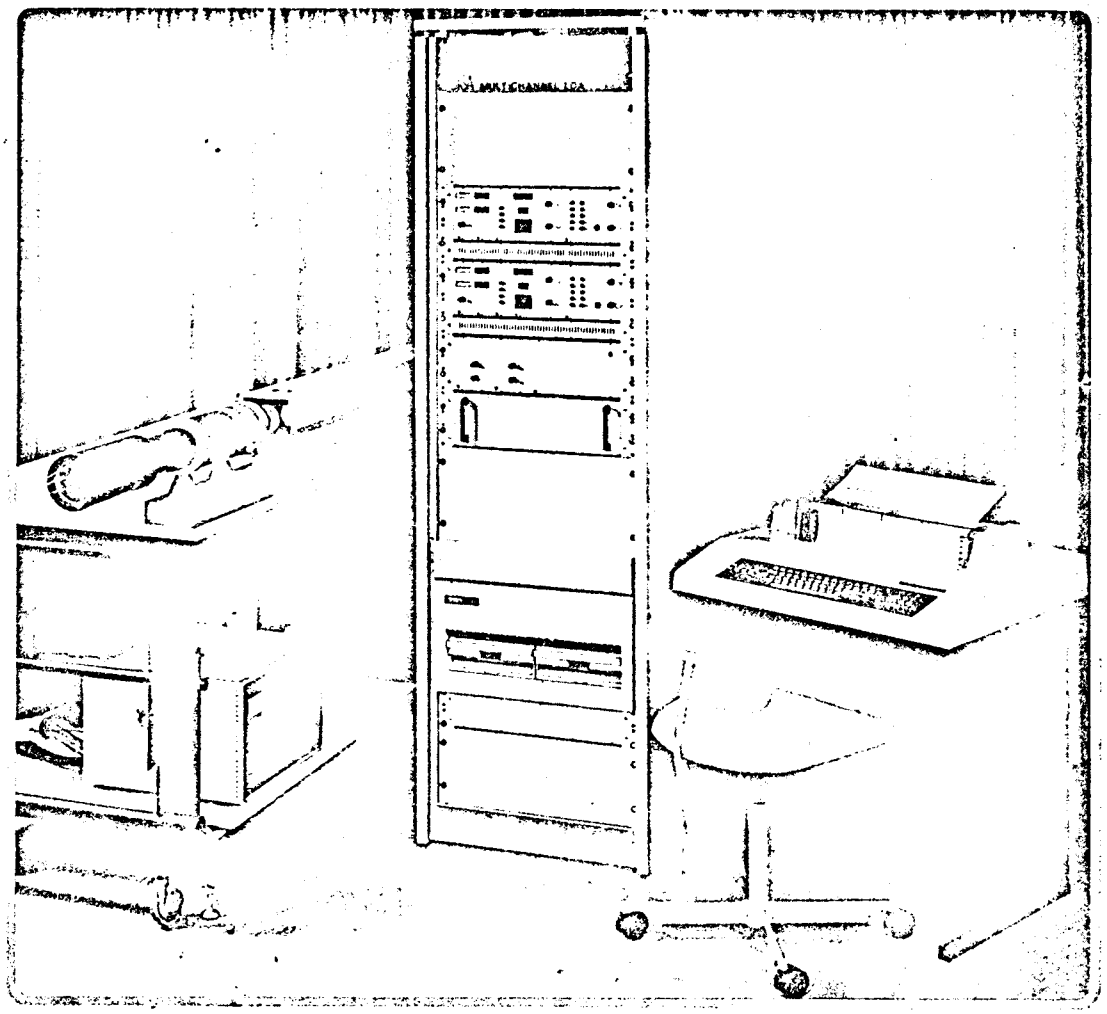

Figure 2. Signal processing equipment.

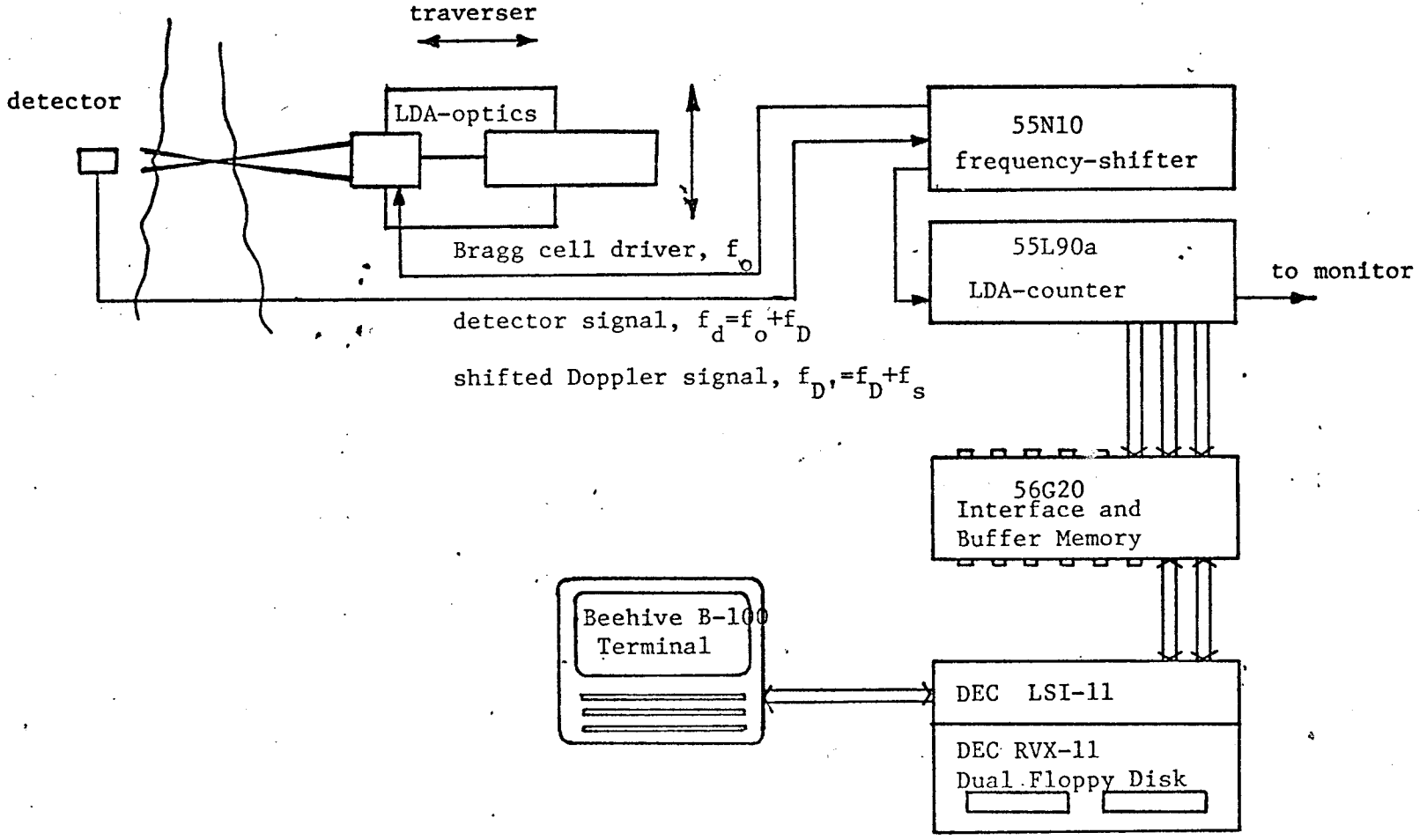

Figure 3. Block diagram of signal processing equipment.

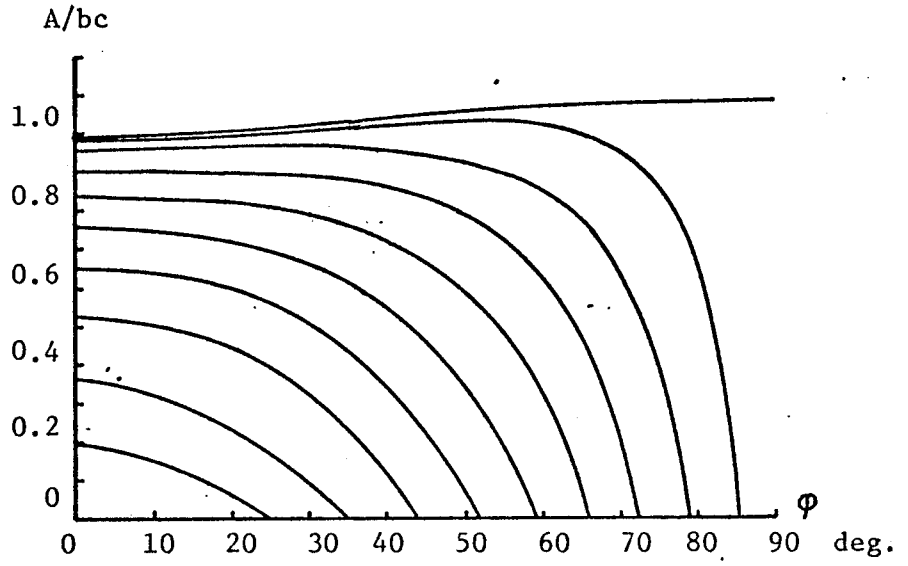

Figure 4. Measuring volume cross section as a function of angle φ in the x-y-plane. ($\theta = 45^{o}$)

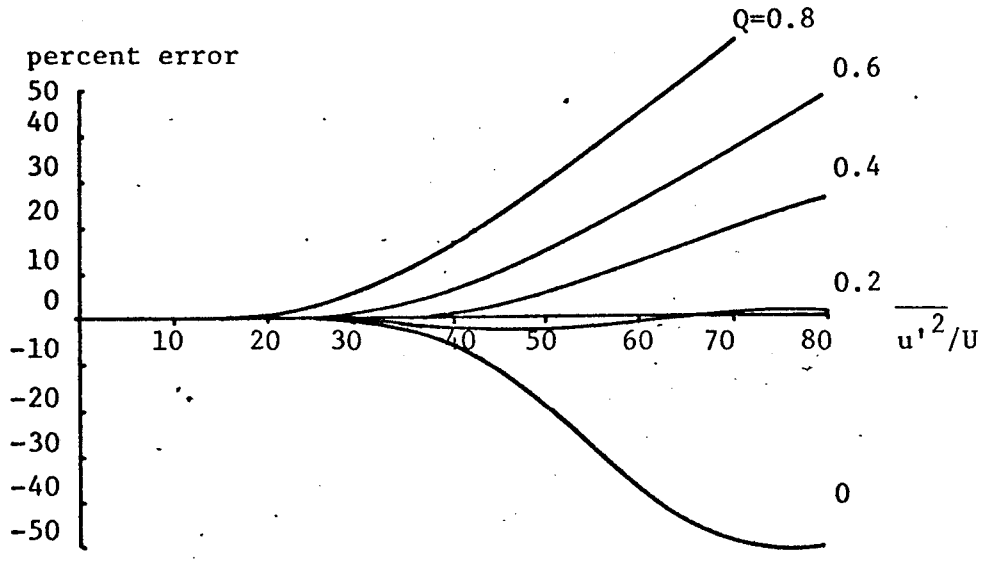

Figure 5. Calculated bias error in mean velocity of 3-D Gaussian, isotropic turbulence including effect of measuring volume cross section.

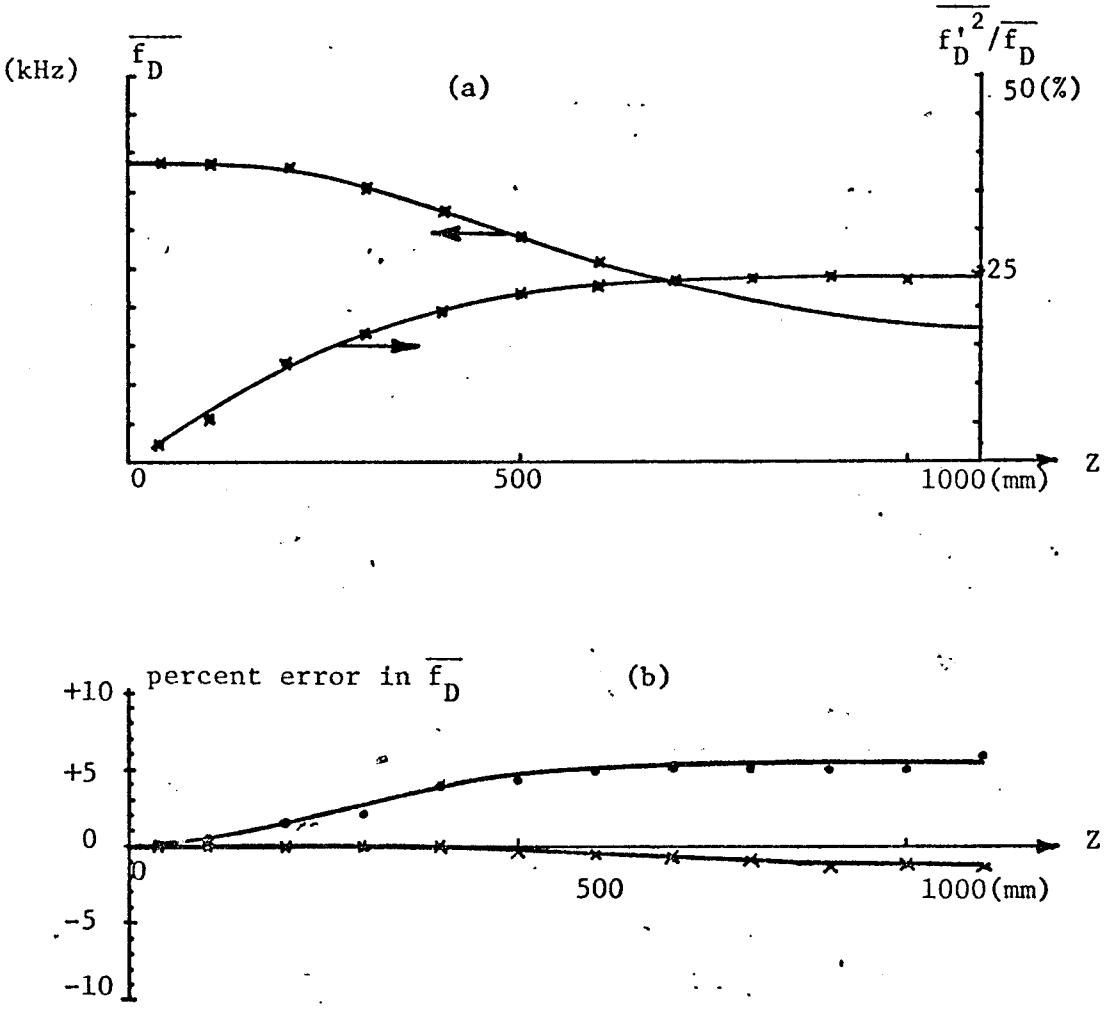

Figure 6. a) Measured axial mean and rms Doppler frequency along jet axis
b) Measured percentage error in mean value relative to residence-time weighted data.

frequency shift 300 kHz

· arithmetic averaging
x 1-D weighted data

(a)

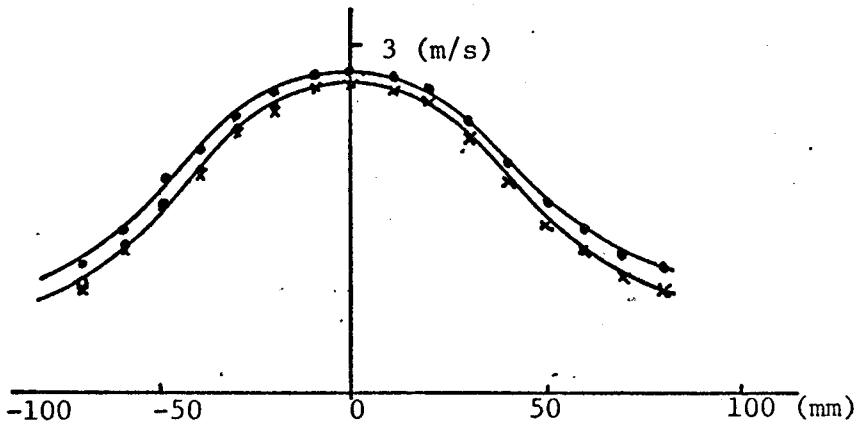

(b)

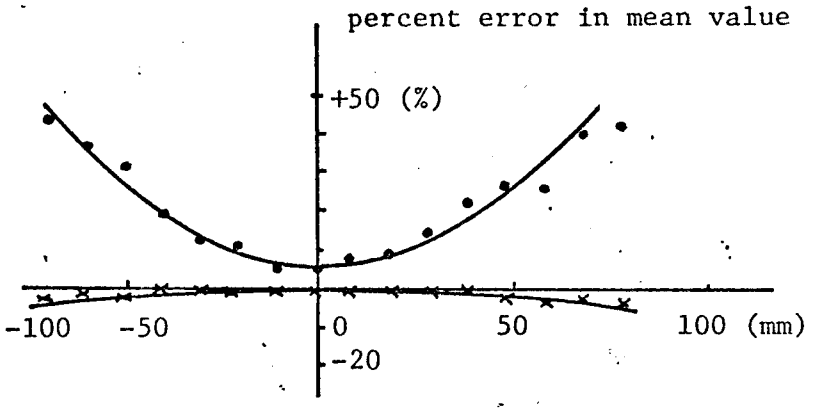

(c)

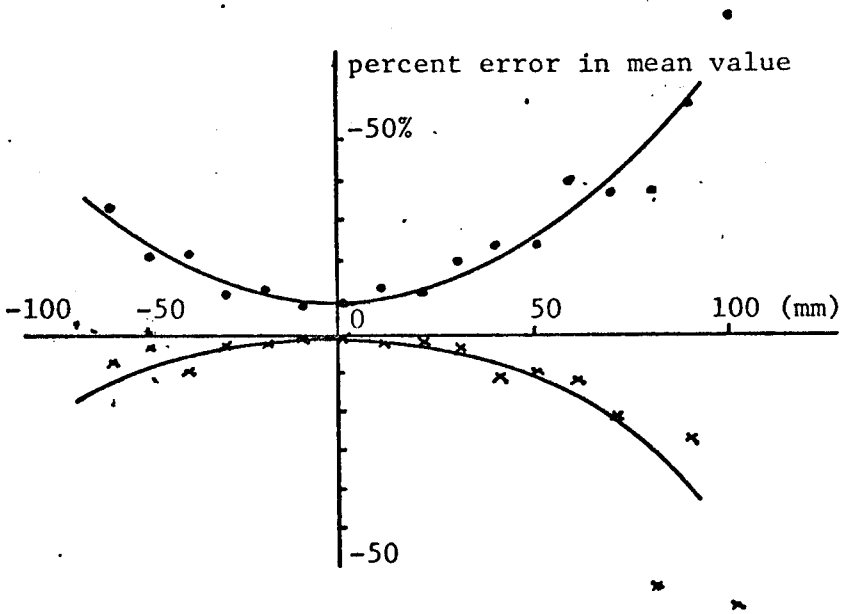

Figure 7. a) Measured axial mean velocity, transverse scan at X/D=5.3
b) Errors in mean value relative to residence-time weighted data, frequency shift 0
c) Same as (b) but frequency shift 200 kHz

• Arithmetic averages

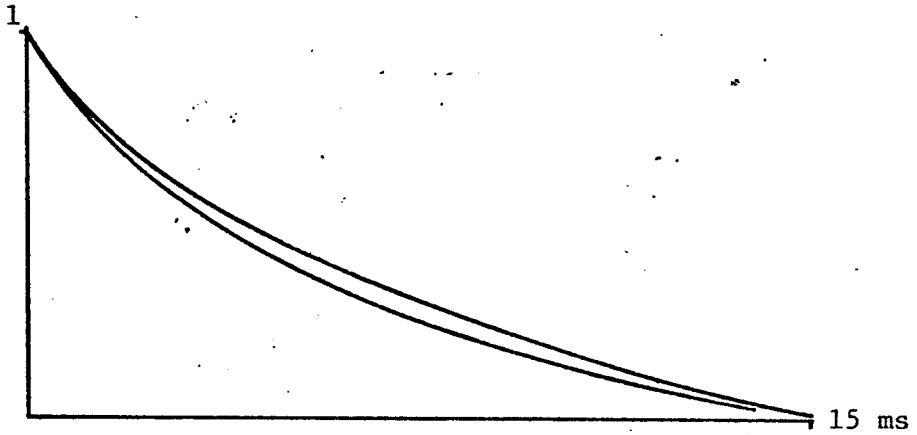

Figure 8. Autocorrelation function of axial velocity at X/D=5.3, 3.25 m/s, frequency shift 200 kHz

Upper curve: arithmetic averaging
Lower curve: residence-time weighted data.